Heliyon 6 (2020) e03807

Contents lists available at ScienceDirect

Heliyon

journal homepage: www.cell.com/heliyon

Research article

Morphological remodeling of the intramural coronary resistance artery network geometry in chronically Angiotensin II infused hypertensive female rats

Anna Monori-Kiss [a], Peter Antal [a], Maria Szekeres [b,e], Szabolcs Varbiro [c], Alexander Fees [b], Bela Szekacs [d], Gyorgy L. Nadasy [b,*]

[a] Institute of Translational Medicine, Semmelweis University, 37-47 Tuzolto Str, H-1094, Budapest, Hungary
[b] Department of Physiology, Semmelweis University, 37-47 Tuzolto Str, H-1094, Budapest, Hungary
[c] Department of Obstetrics and Gynecology, Semmelweis University, 78a Ulloi Str, H-1082, Budapest, Hungary
[d] II. Department of Internal Medicine, Section of Geriatrics, Semmelweis University, 20-22 Halmi Str, H-1115, Budapest, Hungary
[e] Department of Morphology and Physiology, Faculty of Health Sciences, Semmelweis University, 17 Vas Str, H-1088, Budapest, Hungary

ARTICLE INFO

Keywords:
Aging
Pathophysiology
Cardiovascular system
Circulatory system
Physiology
Pathology
Cardiology
Hypertension
Resistance arteries
Network
Remodeling
Angiotensin II
Coronary arteries

ABSTRACT

Segmental remodeling of resistance arteries, inhibition of angiogenetic processes, their rarefaction by AngiotensinII and hypertension are accepted facts. Less is known about alterations in resistance artery network geometry potentially induced by them. Female rats were infused with 100 ng/kg/min AngiotensinII with osmotic minipumps for four weeks that raised mean arterial blood pressure from 98 ± 3 to 125 ± 7 mmHg. Geometry of the left coronary artery system was studied on plastic casts and on in situ microsurgically prepared, saline infused video-microscoped networks (n = 13 and 11 controls and hypertensives, respectively). Parallel running branches, broken course of larger branches, multiple branchings and branch crossings have been identified (13 and 74 such deformities, in control and hypertensive networks, respectively, $p < 0.01$). Bifurcation angles increased with increasing asymmetry of daughter branches but not in hypertensives. Dividing the whole network (theoretically) into several hundreds of 50μm long ring units, ring frequency peaked at 200μm diameter in normal networks. This peak diminished and was replaced by a peak at 300μm in hypertensives ($p < 0.01$). In controls, diameter of vascular units decreased at a fairly even rate with flow distance from the orifice. The 350, 200, 150μm diameter units were found with highest frequencies at flow distances around 2.5, 5.5 and 7.5mm, respectively. This regular pattern disintegrated in hypertensives. Higher blood flow routes were needed to cover the same distance from the orifice ($p < 0.01$). Shrinkage and diminishment of many parallel connected 200μm segments, concomitant enlargement of many larger segments accompanied with morphological deformities can be expected to contribute to elevated vascular resistance.

1. Introduction

Segmental morphological remodeling of resistance arteries in sustained hypertension with thickening of the wall, narrowing of the lumen were classically described by Folkow [1]. Later Baumbach and Mulvany [2, 3] suggested a distinction between hypertrophic and eutrophic wall remodeling. These observations have been confirmed by several authors up to now [4, 5, 6, 7, 8, 9, 10, 11, 12, 13]. In addition to the segmental morphological remodeling process, reduced capillary densities [14, 15, 16, 17] and reduced number of arterioles [7, 12, 17, 18, 19, 20, 21, 22, 23, 24, 25] were found which pointed to *alterations in microvascular networks* in several tissues, ventricular tissue included [6, 26]. "Rarefaction", the term coined by Harper for the reduced number of parallel connected resistance arteries in the tissue [19] gives an explanation for chronically elevated microvascular resistance in addition to the more widely known segmental narrowing-wall thickening. Rarefaction of resistance arterioles in hypertension, however, could not be demonstrated on the spinotrapezius muscle of spontaneously hypertensive rats [27] or, on ventricular arterioles in severe renal hypertension [28]. Resistance artery network alterations in hypertension seem to be more complex than simple reduction in number of vessels [23]. These studies necessitate further investigations, how the resistance artery system

* Corresponding author.
E-mail address: nadasy.gyorgy@med.semmelweis-univ.hu (G.L. Nadasy).

https://doi.org/10.1016/j.heliyon.2020.e03807
Received 13 September 2019; Received in revised form 3 March 2020; Accepted 16 April 2020

geometry is affected during chronic hypertension. Our hypothesis was, that substantial network alterations would be found.

Deteriorated angiogenetic processes have been suspected to be in the background of microvascular rarefaction in essential hypertension [29]. Both in genetically hypertensive (Dahl's salt sensitive) [30] and in genetically diabetic (Torii strain) [31] rats, a suppressed coronary capillary angiogenesis by angiotensin II (AngII) has been observed. Finer morphology of the intraventricular resistance artery network of the heart in hypertension, under the effect of elevated AngII, however, has not yet been studied.

The chronic AngiotensinII infusion technique has been chosen to elevate blood pressure, despite the fact that the direct effect on the vascular wall and the effect through the elevated pressure are hard to distinguish.

With a careful microsurgical technique, we succeeded to prepare the whole resistance artery network of the left anterior descendent coronary artery, down to around 80 μm of diameter in excised rat hearts, then perfuse it with saline at physiological pressures and record the picture of the whole network in situ by videomicroscopy [32, 33]. In the present paper we show, how this intramural resistance artery network running underneath the surface of the rat heart, 0.5–1.0 mm deep is altered after 4 weeks of AngiotensinII (AngII) infusion. Networks were studied both during in situ perfusion and on plastic casts. For quantitative analysis, a statistical geometrical technique has been applied we have published earlier for evaluation of the same network in the aged rat [33]. Female rats have been studied, as we wanted to compare our results with the segmental studies, made earlier on chronic actions of sexual hormones on resistance vessels.

2. Results

2.1. Basic physiology parameters

Body weight of animals did not differ at termination of study (291 ± 5 vs. 297 ± 7 g, for control and AngII infused female animals, respectively). Mean arterial blood pressure and heart weights were significantly elevated in chronically Angiotensin II treated animals (from 98 ± 3 to 125 ± 7 mmHg and from 0.93 ± 0. 01 to 1.06 ± 0.05 g, $p < 0.01$ for both comparisons).

2.2. Morphological abnormalities found in chronically hypertensive networks

The shape of the hypertensive networks had a different appearance (Figure 1b, e, f, g, h and i.) when compared with normal networks (Figure 1a, c and d) both on plastic casts and on microsurgically prepared, in situ perfused networks. This “old tree” appearance was elicited by certain well definable morphological features rarely found in normal (young) networks. These are, the broken course of a larger branch (i), multiple branchings, that is more than two daughter branches emerging from the same or closer point of the mother branch (ii), parallelly, closely running larger branches (iii), crossings of branches upon each other (iv) resulting in mutually exchanged supplying areas, as well as uneven diameter of a segment (v). The statistical distribution of the first four deformations is shown in Table 1. The deformations themselves are

Table 1. Pooled number of morphological deformities found in the resistance artery network of the left anterior descendent coronary artery of normotensive and AngII infused hypertensive female rats.

Morphological deformity	Control normotensive (n = 13)	AngII infused hypertensive (n = 11)	Khi^2 probe significance level
Parallel running	3	17	$p < 0.01$
Broken course	3	20	$p < 0.01$
Multiple branching	6	15	$p < 0.05$
Crosses	1	22	$p < 0.01$
Sum of all deformities	**13**	**74**	**$p < 0.01$**

Significant below $p < 0.05$.

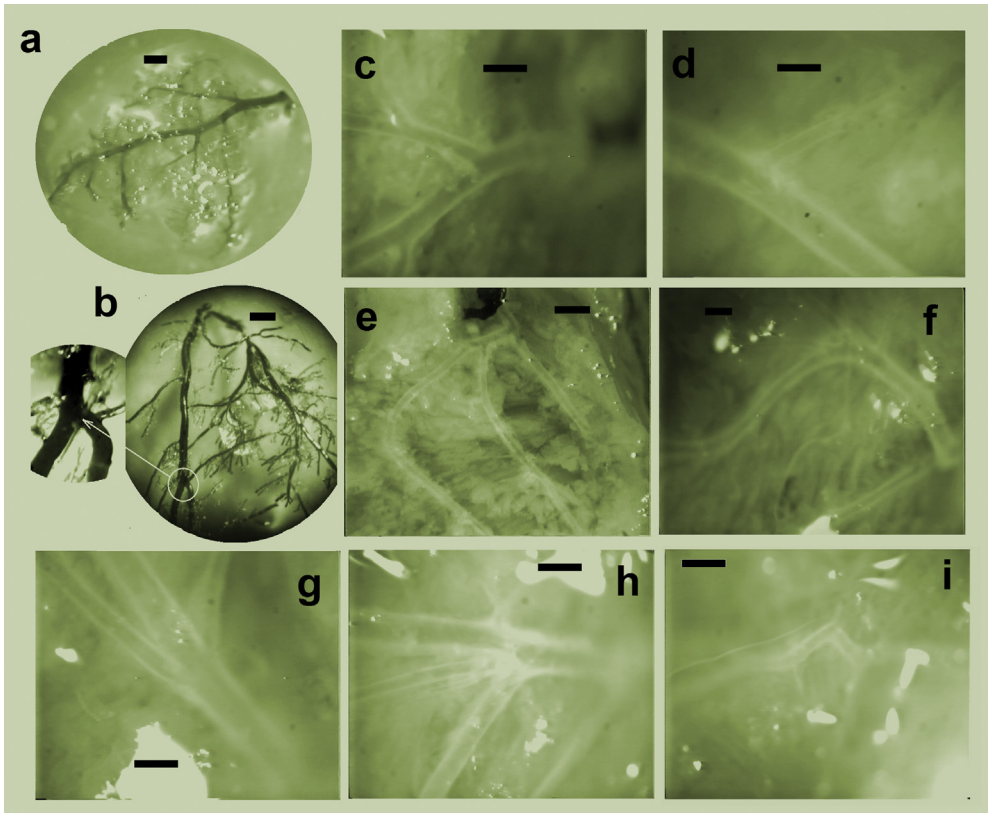

Figure 1. Morphological abnormalities in hypertension a. Control network, plastic cast. b. Hypertensive network, plastic cast. Note undulating course, crossed branches, multiple branching (enlarged in insert). c. and d. Control network, in situ saline perfusion. e. through i. Hypertensive in situ perfused networks. Note broken course of a large branch and parallelly running branches (e), broken course of a large branch and multiple branching (f), multiple branchings (g,h) as well as broken course and uneven diameter (i). Bars, a,b,e, 1000 μm, c,d,f,g,h,i, 500 μm.

demonstrated in Figure 1. There were significantly more of such deformations in the hypertensive networks ($p < 0.01$ and 0.05 with the χ^2 probe).

2.3. Branchings ("bifurcations")

Resistance artery diameters from both the normal and the hypertensive networks fairly well adhered to the Murray principle [34]: the sum of the cubes of the diameters of the daughter branches was close to the cube of the diameter of the mother branch (Figure 2a). There was a difference, however, in the interdaughter angle. In normal networks, this angle significantly increased with increasing asymmetry of the daughter branch diameters ($p < 0.05$ with the Pearson correlation). Such interconnection was missing in hypertensive branchings (Figure 2b) When the deviation of the angle of the larger daughter branch from the course of the mother branch was plotted on a 3D diagram, against its own diameter and against the mother branch's diameter, this revealed partially separated populations (Figure 2c).

2.4. Segments

Number of segments (straight or curved cylindrical stretches erecting very small branches only in-between two bifurcations) was significantly reduced in hypertensive networks in the 150–275 μm diameter range, while it was increased between 275-375 μm (the two distributions being significantly different with the χ^2 probe, $p < 0.01$, Figure 3a). The mean lengths of the segments also changed, it was much reduced in hypertensives between 325-425 μm ($p < 0.05$ with anova, Figure 3b).

2.5. Ring unit analysis

When pictures of networks were divided into 50 μm long ring units, the number of rings characteristically peaked at 200 μm diameter in control networks. However, this peak was missing in hypertensives. Instead, two new peaks, one around 300 μm and one at 425–575 μm diameter, have developed (different with the χ^2 probe, $p < 0.01$). For each ring unit, the direct distance from the orifice and the somewhat larger flow distance (the length of the route of blood flow from the orifice to the given ring) was determined. The differences of these values are plotted on Figure 3d which demonstrates that in hypertensive networks, flow should cover a significantly larger "flow distance" to reach a certain "direct distance" from the orifice than in normal networks. An even deeper insight into the events of network remodeling is offered by the 3D plot, a two dimensional histogram, on which ring unit frequency (color coded) is plotted against both diameter and flow distance. Not surprisingly, in normal networks, smaller arteries are usually in a farther flow distance from the orifice. Frequency clusters of 350, 200, 150 μm diameter units with flow distances around 2.5, 5.5 and 7.5 mm, respectively, laying along a linear line on the diagram were characteristic. However, this fairly coherent pattern has been disorganized in hypertensively remodeled networks. They disappeared and were partially replaced by high number of ring units with diameters of 300 μm in the whole 2.5–10.5 mm flow distance range (Figure 4).

3. Discussion

We have found that four weeks moderate angiotensin infusion and consequent blood pressure elevation induced characteristic alterations in the geometrical properties of the intramural coronary resistance artery network of the rat. Morphological deformations, rarely seen in normal networks appeared, such as broken course of a larger branch, branches running parallel for a longer course, branchings with multiple daughter branches emerging very close to each other, branches crossing each other, with potentially mutually exchanged supplying areas and sometimes uneven diameter. It is plausible that all these alterations disturb normal laminar flow and some way increase vascular resistance. These deformations give an "old tree" appearance to the network (Figure 1 and Table 1). Branch angles also did change. In the normal network, large

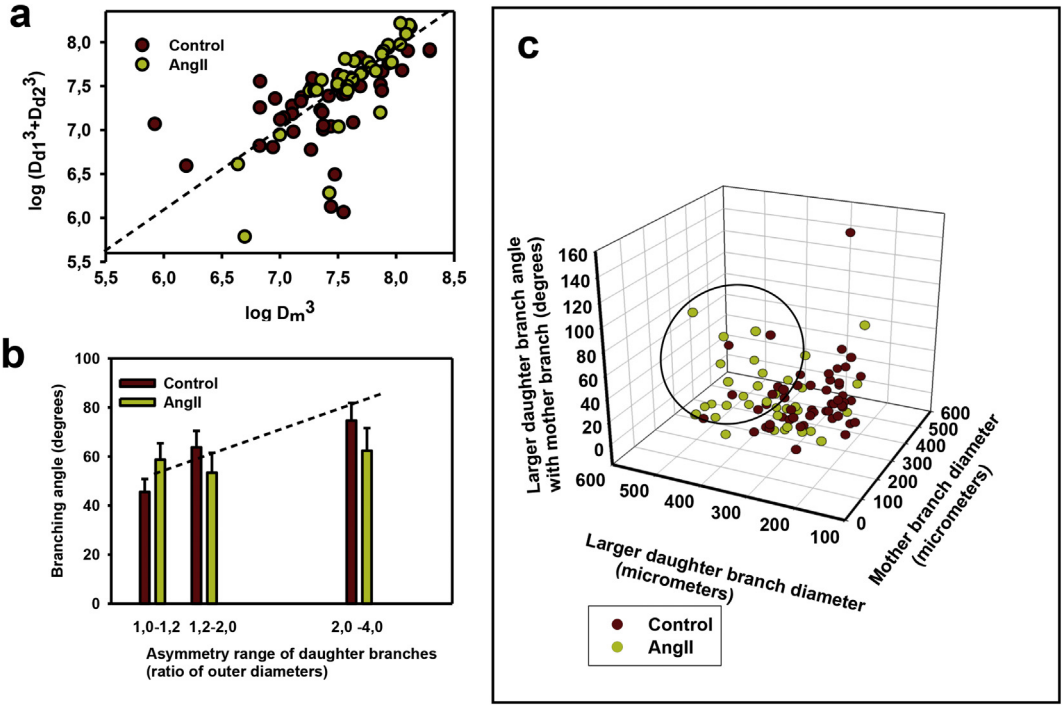

Figure 2. Analysis of branchings a. Sum of the cube of daughter branch diameters plotted against the cube of the diameter of the mother branch. Bifurcations obeying the Murray law are located on the dotted line. Unaffected by hypertension. b. Interdaughter angle as a function of bifurcation asymmetry. Note that branching angle significantly increases with asymmetry in controls only (with Pearson correlation, $p < 0.05$). c. Deviation of the axis of the larger daughter branch from that of the mother branch as a function of diameters. Note that in case of larger branches larger deviation of the daughter branch is more frequently found in hypertensives (marked by the ellipse).

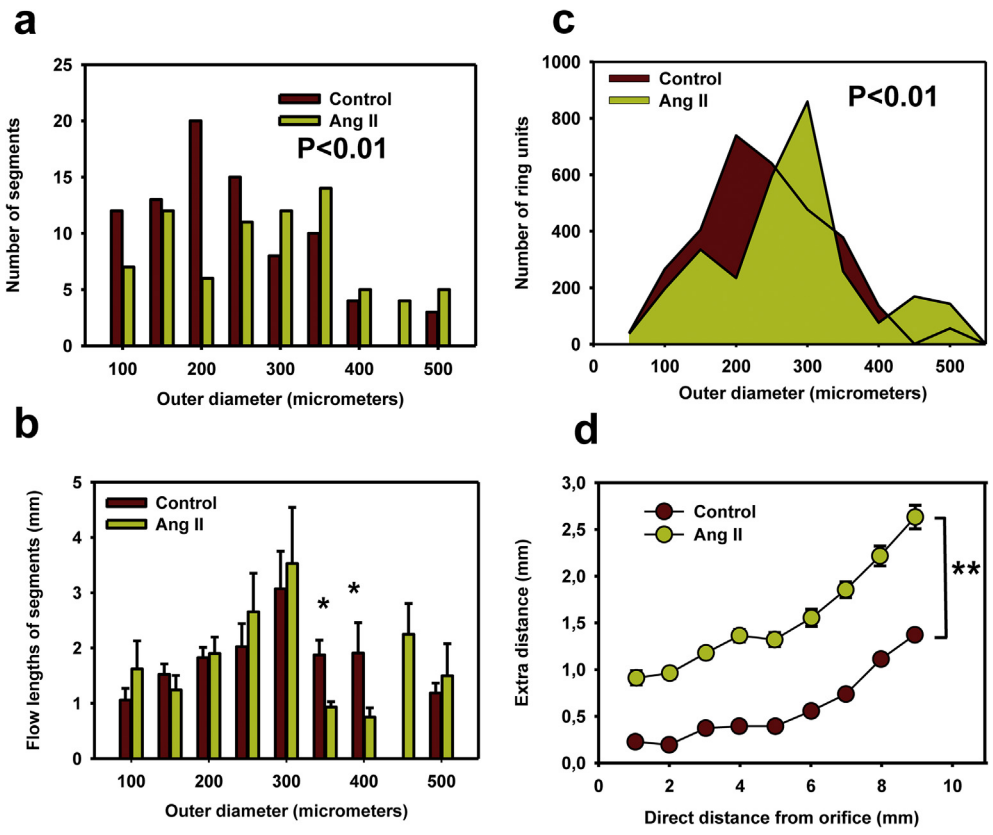

Figure 3. Analysis of segmental and ring units. a. Number of segments with diameters in different ranges. Pooled data, normalized for 6-6 rats. Note reduced number of segments in the 200–250 μm range in hypertensives. Significantly different with the χ^2 probe ($p < 0.01$). b. Mean segmental length as a function of diameter. Note that short but thick segments are most frequently found in hypertensive networks ($p < 0.05$ with anova). c. Number of 50 μm ring units in different diameter ranges. Note reduced number of rings in the 200μm, increased number in the 300 μm range in hypertensive networks. Normalized for 6-6 rats. Significantly different with the χ^2 probe ($p < 0.01$). d. The diagram shows the difference of flow distance and direct distance from the orifice for ring units. Note that in hypertensive networks, substantially more distance should be covered by blood flow to reach a certain direct distance than in normal ones ($p < 0.01$ with two-way anova).

daughter branches are inclined to follow the course of the mother branch, hardly deviating from its axial direction, while smaller branches can emerge almost perpendicularly. An opposite situation is not infrequent in remodeled networks, causing the visibly broken course of larger branches. One is inclined to think that it has been formed from an asymmetric branching: by morphological widening of the lumen of the perpendicular original thin branch and thinning of the lumen of the originally thicker daughter branch. The existence of such diminishing "ghost arterioles" was suspected by LeNoble two decades ago [29]. The diameter rearrangement can be seen on Figure 3a. It shows the loss of 200–250 μm diameter segmental elements. The ring frequency plot of Figure 3c suggests that some of them could have been closed and lost forever as parallelly connected resistance units, while others increased in diameter and joined the 300 μm population (Figure 3a and c). That means the reduced number of parallel connected 200 μm diameter elements. The appearance of a 450–500 μm population can be connected to increased coronary flow due to elevated heart work and axial elongation due to elevated heart mass. It is almost sure that such new elements have been formed from the original 350–400 μm diameter populations. Figure 3b suggests that especially the longer 350–400 μm diameter segments were inclined to dilate, reducing this way the mean lengths in the original population. An even more detailed picture of the network

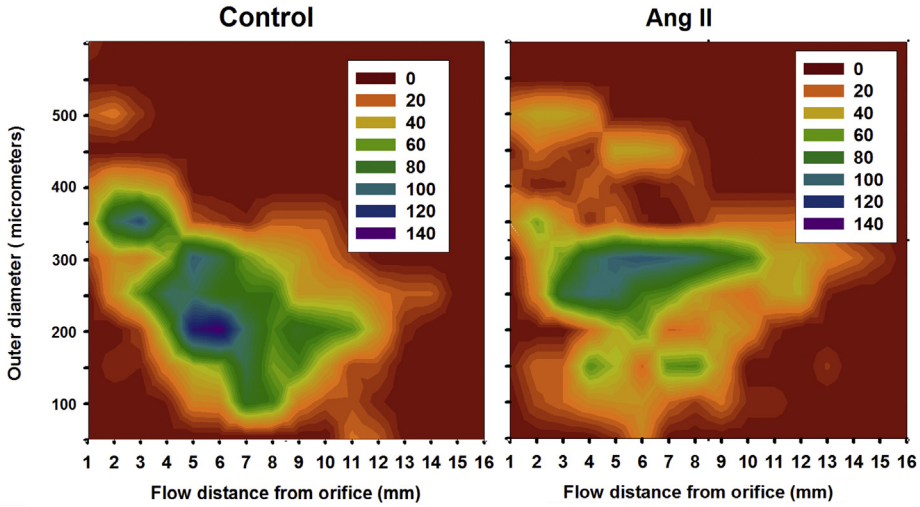

Figure 4. Ring unit frequency (color coded) for different diameters and flow distances from the orifice: a two-dimensional histogram. Note that in normal network, smaller arteries are usually farther from the orifice. This pattern has been lost in hypertensive segments: 300 μm arteries dominate the 3–10 mm flow distance range, while the population of 200 μm vessels disappeared.

remodeling events can be read from the 3D plot of Figure 4. With all probability, the clusters of 500 and 450 μm units have been formed by dilation and some elongation from the 350 μm cluster of the control network which fully diminished. The originally determining 200 μm cluster (at 4–8 mm flow distance) practically disappeared. Some remnants might shrunk to 150 μm forming a new cluster (at 4 mm). A smaller portion of 200 μm vessels could have dilated, forming the strengthened 300 μm population which now extends toward an unusually far, 12 mm distance.

Our observations are in good accordance with several earlier ones, and yield, in many respect, a deeper insight into the events of coronary resistance artery remodeling processes. Elaborate studies on the intramural resistance artery network remodeling in ventricular hypertrophy elicited by the ascendant aortic stricture technique have been published by Kassab [35] and by Huo [36]. Geometrical alterations have been analyzed on plastic casts. They have found that number of segments increased, while their length decreased. For analysis they divided the segments according to their order of branching. Our and others' [37] experience is that asymmetric branchings are very frequent in the coronary resistance artery network, an approach to the network geometry through branching order of segments will thus yield vessels with very diverse calibers. Another technique is offered by the chaos theory and computing the scalarity of the network [38]. That approach is based on the assumption that there are geometric analogies in the network mapped at lower and higher scalar magnification (analogy of minute parts with the whole). Similar principles are governing vascular network development during different phases of embryonic and postnatal development, however, hemodynamic functions of vessels with different calibers, those located at different distances from large, high-pressure, pulsating vessels will have several independent components influencing network development. In a previous publication [33], we used a new computational technique: the whole subsurface, intramural network of the left anterior descendent coronary artery of the rat was divided into ring units, uniformly with 50 μm length and networks characterized with diameter frequencies of such ring units in different direct and flow distances from the orifice. Such a plot is shown for normotensive and hypertensive networks on Figure 4. The comparison clearly shows that in the normal network, typical diameters almost linearly decrease with flow distance from the orifice. This pattern, however, is disintegrated in the hypertensively remodeled networks. Analysis of Figs. 3c and 4 shows that part of the population of 200 μm vessel units diminished while another part of them dilated to 300 μm Fig. 3a and b demonstrate, that it is really the number, not the length of the 200 μm segments, which have been affected. Many of the originally 300–400 μm main branch segments (located close to orifice) dilated to 450–550 μm (see top two spots on the right panel of Figure 4.). Figure 3b suggests that the shorter ones of this population remained. Inside the ventricular tissue branch angle alterations cannot easily happen because of the hindrance caused by the ventricular tissue itself. However, a massive rearrangement of (morphological) segmental diameters can easily be accomplished. Normally, larger daughter branches tend to follow the direction of the mother branch, while tinier daughter branches can arise almost perpendicularly: interdaughter branch angle increases with asymmetry of the daughter branches. This pattern can be recognized on the normal network (Figure 2b and c). Morphological dilation of a narrow daughter artery rising almost perpendicularly will result a larger diameter vessel branching away at a large angle unusual for its diameter. If the original larger branch fully diminishes, forming a "ghost arteriole" [29], the picture of a larger artery with a broken course will emerge (Figure 1b, e, f and i). Figure 5 gives an explanation how the observed geometrical alterations could have originated from morphological shrinkage and dilation of different elements of the originally existing network.

Tortuosity of retinal small arteries was found by Bhutto [39] in hypertensive rats on casts. Such a morphological deviation can be supposed to increase difference between flow route and direct distance as shown on our Figure 3d. No arteriolar rarefaction has been found on the spinotrapezius arcade vessels in SHR by Engelsson [27], in fact the number of such vessels seemed to be even more abundant. Our studies show that in coronaries of Ang II infused rats, rarefaction affects only characteristic diameter ranges in the network (Figures. 3a, c and 4). In coronary vessels, Rodriguez-Martinez also did not find any rarefaction in renovascular hypertension of pigs [28]. Henrich [20] found in SHR rat mesenteric arterioles, in addition to rarefaction a shortened length. A shortened length could be proven by us in the small artery (350–400μm) diameter range in our studies (Figure 3b). However, our analysis (see above) shows that this is the result of diameter rearrangement, not a real reduction of length. Zamir [40] described that at arterial bifurcations, smaller daughter branches formed larger angle with mother artery than did the larger daughter branches. That law seems to be disturbed in hypertensive networks. In our Figure 2b it can be observed, that interdaughter angle increases with increasing diameter asymmetry of the daughter branches in the control arteries but not in the hypertensives. In addition, on the 3D plot of Figure 2c, a new population of points appears, representing the large daughter branches directed away from mother branch at a higher degree (encircled). It is an interesting observation that hypertensive branchings still seem to adhere the Murray law [34], according to the sum of the diameter cubes of the daughter branches is equal with the cube of the diameter of the mother branch (Figure 2a). Stabilization of endothelial shear is the explanation [41, 42]. The Murray law remains valid, despite the fact that damaged endothelial dilation ability is present in all vessels in hypertension [11].

Reduced number of capillaries on a tissue cross section by all probability marks reduced potential for oxygenation. However, in case of resistance arteries, the situation is much more complex. A reduced number of arteriolar cross-sections can mean either increased or reduced resistance, according to whether the number of parallelly connected segments is reduced or the length of segments (serially connected resistance units). From the hemodynamic point of view, it is plausible that the morphological aberrations shown on Figure 1 and listed in Table 1 disturb cylindrical geometry, increase vascular resistance, even potentially may disturb laminal flow. Figure 3d demonstrates that flow routes are significantly elevated in the network which also increases resistance. While morphological dilation could be demonstrated in larger branches close to pulsating pressure of the orifice, a substantial reduction of number of segments in the 200 μm means a much higher hemodynamic resistance until that point of the ventricular circulation. We have to admit, that even more important resistance vessels are located below that diameter level, which could not covered by our study. Clinically, elevation of resistance is not unanimously a damaging, it can even form an adaptive factor saving smaller vessels from pressure load and preventing elevated capillary pressure. However, such morphological alterations will make it difficult to restore normal arterial pressure and tissue flow.

It is interesting to compare these observations on the chronically hypertensive coronary resistance artery network with earlier one made by us on *non-hypertensive aging* (male) rats using a similar technique [33]. Broken course and triple branchings were frequent observations also in aged rats, as were the extended flow length, similar irregularities of branching angles with maintenance of the Murray law of diameters and an almost identical rarefaction of the network in the 200μm diameter units. *Certain similarities between the aging and hypertensive remodeling processes are prominent.*

Acute vasodilator action is the main mechanism of many antihypertensive drugs applied today. There is a good reason to think that reduction of blood pressure achieved by them prevents or maybe, even reverses morphological hypertensive remodeling of resistance vessels [9, 17]. A better understanding of the hypertensive network remodeling process may lead us closer to devising new therapies directly preventing or even restoring the disturbed resistance artery network morphology by influencing the angiogenetic processes.

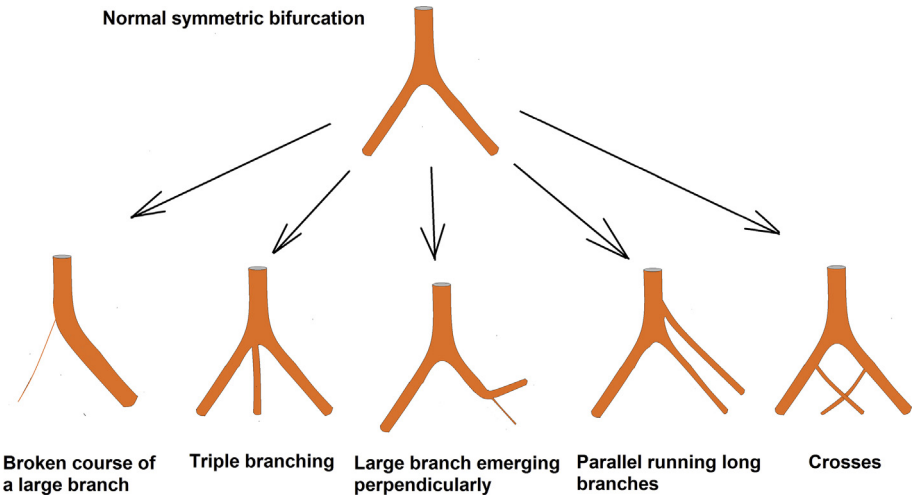

Figure 5. Explanation how the observed geometrical deformities in the hypertensive network could have developed from the original network simply due to morphological shrinkage of certain larger branches while morphological dilation of some microcirculatory units.

4. Conclusions

Substantial geometrical remodelling does occur in the intramural coronary resistance artery network with chronic hypertension. The observed abnormalities, broken course of a larger branch, triple branchings, larger branches emerging perpendicularly, parallel running branches and branches crossing each other resemble to those found earlier in the elderly network. Disturbed hemodynamics and reduced number of parallel connected arterioles in the 150–250 μm (outer) diameter range (rarefaction) can be important components in the elevation of the local hemodynamic resistance. We are convinced that these whole network geometry changes, from hemodynamical point of view, are at least as important as the more widely studied alterations of large coronary arteries and small artery segmental changes. Our observations also shed some light onto the mechanism of this nondescribed yet geometrical network remodeling. Unfortunately it predicts, that local molecular events will be different at different sites of the network: both proliferative and regressing changes being present at the same time at sterically different points of the network. This further complicates their study at the cellular and molecular level.

5. Materials and methods

5.1. Animals

For the experiments, female Sprague-Dawley rats were chosen, aging 8–9 weeks, weighing 260 ± 7 g at the start of the study. In 11 rats in Nembutal anesthesia (45 mg/kg body weight, intraperitoneally) an ALZET osmotic minipump (2ML4) was inserted underneath the back skin, filled with angiotensin II (Sigma), diluted in saline. This ensured an approximately 100 ng/min/kg body weight infusion, somewhat decreasing with weight gain of the animals. That dose has been found in earlier studies statistically significantly elevate blood pressure without devastating strokes and kidney damage to occur. Thirteen additional female rats from the same series were sham operated, with plastic tubes of similar size inserted underneath the back skin and were kept as parallel controls. After 4 weeks the animals were reanesthetized, hearts removed, their weight measured. ILAR prescriptions and local Euro-conform regulations have been adhered to throughout the experiments. They have been approved by the University's Animal Care Committee and state authorities (PEI/001/821–2/2015).

5.2. In situ perfusion and video-microscopy

The whole intramural subsurface network of the left anterior descendent coronary artery was prepared in 8 hypertensive and 8 control rats. Hearts were pinned frontal face up to the bottom of a Petri dish, filled with cooled normal Krebs-Ringer solution to slow down cellular metabolism during the preparation process. Microsurgical preparation was made under a zoomed preparation microscope (Wild M3Z) with sharpened micro-forceps and disposable injection needles. The main branch and its end- and side branches were followed toward the periphery toward vessels with 80 μm outer diameter [32]. In the rat heart, the main branch of the left anterior coronary artery immerses into the ventricular tissue after about 1–2 mm length from the orifice, the main branch and its larger branches then run under the surface, mostly parallel with it, embedded 0.5–1 mm deep in the ventricular tissue. Smaller branches penetrate the ventricular wall. Ventricular tissue and loose connective tissue were removed from upper and side surfaces of the coronary arteries, the contact with ventricular tissue at the bottom and emerging smaller side branches were left intact. Larger branches running under the surface were followed further distally. This ensured a practically unaltered in situ geometry of the network [32] (Figure 1). Then the orifice was cannulated with a microcannula (400 μm of outer diameter) and pressurized to 100 mmHg. Tissue bath and perfusing solution were normal Krebs-Ringer solutions, warmed to 37 °C, bubbled with a gas mixture of 20% O_2, 5% CO_2 and 75% N_2 which kept pH at 7.4. The composition of the solution we used was: NaCl 119, KCl 4.7, NaH_2PO_4 1.2, $MgSO_4$ 1.17, $NaHCO_3$ 24, $CaCl_2$ 2.5, glucose 5.5, and EDTA 0.034 (all in mmol/lit).

Videomicroscopic images (Leica DFC 320 camera, Leica QWin software) with low and high magnifications were taken from the vertical direction and also with microscope angle bent to about 30° from vertical to visualize sides and apex. Pictures of a micrometer etalon (Wild) were made for each magnification.

5.3. Plastic casts

In the remaining (5 control and 3 hypertensive) rat hearts the orifice was cannulated, and Batson17 plastic solution was injected into the coronary system. After hardening, the tissue was digested away in KOH as described by the manufacturer. Plastic casts of the networks were studied under the preparation microscope (Wild M3Z), arteries were prepared clear of surrounding veins and smaller vessels and photographed.

5.4. Image analysis

From the pictures taken the whole network can be reconstructed flattened into the horizontal plane. The ensuing 2D geometrical analysis

is much easier than the 3D one. Digitized pictures with final pixel sizes from 31.1 to 5.1 μm (lowest/highest magnifications) were further analyzed. At inspection, it turned out that hypertensive networks frequently had morphological abnormalities, such as closely, parallel running branches, the broken course of a larger branch, multiple branchings (e.g. "trifurcations"), branches crossing over each other (See Figure 1 and Table 1). Such abnormalities were identified and counted both on perfused networks and on plastic casts by a blinded observer. Perfused segments were subjected to a more detailed geometrical analysis. Orifice, apex, axis of branch segments, points of branchings have been identified on composite pictures at high and low magnifications. Segments were consecutively numbered, their outer diameter measured at several places. Segmental analysis was performed by constructing a list of all segments, containing their direct length, bent length and diameter. A list of all branchings ("bifurcations") was constructed containing the diameters of the mother and daughter branches, deviation of the daughter branch from the axis of the mother branch in degrees, and the angle between the daughter branches. Then, according to our previous image analysis technique [33] a Cartesian coordinate system was constructed for each heart, with X axis starting at the orifice and drawn toward the apex, while the Y axis was drawn perpendicular to the X axis through the orifice, with positive Y values toward the anatomical left. Photographs taken at tilted angle from lateral and apical curvatures were fitted back to the horizontal plane. Then the whole network was theoretically divided into cylindrical ring units, uniformly with 50 μm axial length. Each ring unit was characterized by its diameter, angle of its axis with the X axis, and XY coordinates (of its center). Direct distance from the orifice and the "flow distance" (the length of flow route from orifice to the given ring unit) were separately computed for each. As a sum, 100 and 78 segments, 44 and 34 bifurcations as well as and 3669 and 2902 ring units were identified and analyzed for 7 control and 6 hypertensive networks, respectively.

5.5. Statistics

Morphological abnormalities were counted and pooled for all perfused networks and casts by blinded observer. Their number was tested with the χ^2 probe. The same statistical test was used to compare number of segments and ring units in a certain diameter range. Segmental lengths were compared with anova. Pearson correlation revealed interconnection between asymmetry of bifurcations and branch angle. A 3D scatter plot reveals differences in daughter branch angle as a function of diameter. Interconnections between flow distance from orifice and vascular ring diameter as well as number of rings observed in the given ranges of these two parameters were analyzed on 3D plots of two-dimensional histograms.

Declarations

Author contribution statement

A. Monori-Kiss and G. Nadasy: Conceived and designed the experiments; Performed the experiments; Analyzed and interpreted the data; Wrote the paper.

B. Szekacs and S. Varbiro: Conceived and designed the experiments; Analyzed and interpreted the data.

M. Szekeres: Performed the experiments.

A. Peter: Analyzed and interpreted the data.

A. Fees: Analyzed and interpreted the data; Wrote the paper.

Funding statement

This work was supported by Hungarian National Grants OTKA TO32019 and NKFIH K116954, The Hungarian Hypertension Society, The Hungarian Kidney Foundation and by a grant from the Dean of the Medical Faculty, Semmelweis University Budapest. A. Fees was supported by the Fulbright Stipend.

Competing interest statement

The authors declare no conflict of interest.

Additional information

No additional information is available for this paper.

Acknowledgements

†Professor Emil Monos MD, PhD, DSci deceased on the 19th Nov 2018 while shaping the paper with His contribution was in progress. We offer this paper to His Dear Memory. Andrea Simon MD and Erika Szalai MD provided valuable help at construction and analysis of network pictures. We want to express our gratitude to prof Csaba Farsang, MD, PhD, DSci who read a preliminary form of the paper and gave many useful advice how to improve it. The expert technical assistance to Oraveczné Muranyi Ildiko is thanked.

References

[1] B. Folkow, The haemodynamic consequences of adaptive structural changes of the resistance vessels in hypertension, Clin. Sci. 41 (1971) 1–12.
[2] G.L. Baumbach, D.D. Heistad, Remodeling of cerebral arterioles in chronic hypertension, Hypertension 13 (1989) 968–972.
[3] M.J. Mulvany, G.L. Baumbach, C. Aalkjaer, A.M. Heagerty, N. Korsgaard, E.L. Schiffrin, D.D. Heistad, Vascular remodeling, Letter) Hypertension 28 (1996) 505–506.
[4] K. Rakusan, P. Wicker, Morphometry of the small arteries and arterioles in the rat heart: effects of chronic hypertension and exercise, Cardiovasc. Res. 24 (1990) 278–284.
[5] B. Folkow, "Structural factor" in primary and secondary hypertension, Hypertension 16 (1990) 89–101.
[6] R.J. Tomanek, M.R. Aydelotte, C.A. Butters, Late-onset renal hypertension in old rats alters myocardial microvessels, Am. J. Physiol. Heart Circ. Physiol. 259 (1990) H1681–H1687.
[7] J.C. Vitullo, M.S. Penn, K. Rakusan, P. Wicker, Effects of hypertension and aging on coronary arteriolar density, Hypertension 21 (1993) 406–414.
[8] S. Varbiro, B. Szekacs, G.L. Nadasy, N. Acs, Z. Miklos, A. Tokes, E. Monos, Effect of ovariectomy and hormone replacement therapy on small artery biomechanics in angiotensin-induced hypertension in rats, J. Hypertens. 18 (2000) 1587–1595.
[9] G.L. Nadasy, S. Varbiro, M. Szekeres, A. Kocsis, B. Szekacs, E. Monos, M. Kollai, Biomechanics of resistance artery wall remodeling in Angiotensin-II hypertension and subsequent recovery, Kidney Blood Pres. Res. 33 (2010) 37–47.
[10] G. Grassi, R.E. Schmieder, The renaissaince of the retinal microvascular network assessment in hypertension: new challenges, J. Hypertens. 29 (2011) 1289–1291.
[11] A. Yannoutsos, B.I. Levy, M.E. Safar, G. Slama, J. Blacher, Pathophysiology of hypertension: interactions between macro and microvascular alterations through endothelial dysfunction, J. Hypertens. 32 (2014) 216–224.
[12] A. Virdis, C. Savoia, G. Grassi, G. Lembo, C. Vecchione, G. Seravelle, S. Taddei, M. Volpe, E.A. Rosei, D. Rizzoni, Evaluation of microvascular structure in humans: a 'state of the art' document of the Working Group on macrovascular and microvascular alterations of the Italian Society of Arterial Hypertension, J. Hypertens. 32 (2014) 2120–2129.
[13] C. Tsioufis, K. Dimitriadis, N. Katsiki, D. Tousoulis, Microcirculation in hypertension: an update on clinical significance and therapy (Review), Curr. Vasc. Pharmacol. 13 (2015) 413–441.
[14] T.F. Antonios, D.R. Singer, N.D. Markandu, P.S. Mortimer, G.A. MacGregor, Structural skin capillary rarefaction in essential hypertension, Hypertension 33 (1999) 998–1001.
[15] T.F. Antonios, D.R.J. Singer, N.D. Markandu, P.S. Mortimer, G.A. MacGregor, Rarefaction of skin capillaries in borderline essential hypertension suggests an early structural abnormity, Hypertension 34 (1999) 655–658.
[16] A. Prasad, G.S. Dunnil, P.S. Mortimer, G.A. MacGregor, Capillary rarefaction in the forearm skin in essential hypertension, J. Hypertens. 13 (1995) 265–268.
[17] F. Feihl, L. Liaudet, B. Waeber, B.I. Levy, Hypertension, a disease of the microcirculation? Hypertension 48 (2006) 1012–1017.
[18] P.M. Hutchins, A.E. Darnell, Observations of a decreased number of small arterioles in spontaneously hypertensive rats, Circ. Res. 34–35 (suppl 1) (1974) 161–165.
[19] R.N. Harper, M.A. Moore, M.C. Marr, L.E. Watts, P.M. Hutchins, Arteriolar rarefaction in the conjunctiva of human essential hypertensives, Microvasc. Res. 16 (1978) 369–372.
[20] H. Henrich, R. Hertel, Assmann, Structural differences in the mesentery microcirculation between normotensive and spontaneously hypertensive rats, Pflugers Arch Eur J Physiol 375 (1978) 153–160.

[21] M.J. Mulvany, Do resistance vessel abnormalities contribute to the elevated blood pressure of spontaneously-hypertensive rats? A review of some of the evidence, Blood Ves. 20 (1983) 1–22.
[22] A.D. Hughes, E. Martinez-Perez, A.S. Jabbar, A. Hassan, N.W. Witt, P.D. Mistry, N. Chapman, A.V. Stanton, G. Beevers, R. Pedrinelli, K.H. Parker, S.A. Thom, Quantification of topological changes in retinal vascular architecture in essential and malignant hypertension, J. Hypertens. 24 (2006) 889–894.
[23] W.L. Murfee, G.W. Schmid-Schönbein, Structure of microvascular networks in genetic hypertension, Methods Enzymol. 444 (2008) 271–284.
[24] M. Yang, W.L. Murfee, The effect of microvascular pattern alterations on network resistance in spontaneously hypertensive rats, Med. Biol. Eng. Comput. 50 (2012) 585–593.
[25] L. Laurent, P. Boutouyrie, The structural factor of hypertension. Large and small artery alterations, Circ. Res. 116 (2015) 1007–1021.
[26] R.J. Tomanek, P.J. Palmer, G.L. Peiffer, K.L. Schreiber, C.L. Eastham, M.L. Marcus, Morphometry of canine coronary arteries, arterioles, and capillaries during hypertension and left ventricular hypertrophy, Circ. Res. 58 (1986) 38–46.
[27] E.T. Engelson, G.W. Schmid-Schönbein, B.W. Zweifach, The microvasculature in skeletal muscle. II. Arteriolar network anatomy in normotensive and spontaneously hypertensive rats, Microvasc. Res. 31 (1986) 356–374.
[28] M. Rodriguez-Porcel, X.Y. Zhu, A.R. Chade, B. Amores-Arriaga, N.M. Caplice, E.L. Ritman, A. Lerman, L.O. Lerman, Functional and structural remodeling in the myocardial microvasculature in early hypertension, Am. J. Physiol. Heart Circ. Physiol. 290 (2006) H978–H984.
[29] F.A.C. LeNoble, F.R.M. Stassen, W.J.G. Hacking, H.A.J. Struiker-Boudier, Angiogenesis and hypertension, J. Hypertens. 16 (1998) 1563–1572.
[30] H. Yazawa, M. Miyachi, M. Furukawa, K. Takahashi, M. Zakatsu, K. Tsuboi, M. Ohtake, T. Murase, T. Hattori, Y. Kato, T. Murohara, K. Nagata, Angiotensin-converting enzyme inhibition promotes coronary angiogenesis in the failing heart of Dahl salt-sensitive hypertensive rats, J. Card. Fail. 17 (2011) 1041–1050.
[31] T. Masuda, S. Muto, G. Fujisawa, Y. Iwazu, M. Kimura, T. Kobayashi, M. Nonaka-Sarukawa, N. Sasaki, Y. Watanabe, M. Shinohara, Shimada K. Murakami, E. Kobayashi, E. Eiji Kusano, Heart angiotensin II-induced cardiomyocyte hypertrophy suppresses coronary angiogenesis and progresses diabetic cardiomyopathy, Am. J. Physiol. Heart Circ. Physiol. (2012) H1871–H1883.
[32] G.L. Nadasy, M. Szekeres, L. Dezsi, S.Z. Varbiro, B. Szekacs, E. Monos, Brief communication Preparation of intramural small coronary artery and arteriole segments and resistance artery networks from the rat heart for microarteriography and for in situ perfusion video mapping, Microvasc. Res. 61 (2001) 282–286.
[33] E.A. Wappler, P. Antal, S. Varbiro, B. Szekacs, A. Simon, Z. Nagy, E. Monos, G.L. Nadasy, Network remodeling of intramural coronary resistance arteries in the aged rat: a statistical analysis of geometry, Mech. Ageing Dev. 134 (2013) 307–313.
[34] C.D. Murray, The physiological principle of minimum work. I. The vascular system and the cost of blood volume, Proc. Natl. Acad. Sci. U.S.A. 12 (1926) 207–214.
[35] G.S. Kassab, C.A. Rider, N.J. Tang, Y.C. Fung, Morphometry of pig coronary arterial trees, Am. J. Physiol. Heart Circ. Physiol. 265 (1993) H350–H365.
[36] Y. Huo, G.S. Kassab, Compensatory remodeling of coronary microvasculature maintains shear stress in porcine left-ventricular hypertrophy, J. Hypertens. 30 (2012) 608–616.
[37] B. Kaimovitz, Y. Huo, Y. Lanir, G.S. Kassab, Diameter asymmetry of porcine coronary arterial trees: structural and functional implications, Am. J. Physiol. Heart Circ. Physiol. 294 (2008) H714–H723.
[38] C.C. Sng, W.L. Wong, C.Y. Cheung, J. Lee, E.S. Tai, T.Y. Wong, Retinal vascular fractal and blood pressure in a multiethnic population, J. Hypertens. 31 (2013) 2036–2042.
[39] I.A. Bhutto, T. Amemiya, Vascular changes in retinas of spontaneously hypertensive rats demonstrated by corrosion casts, Ophthalmic Res. 29 (1997) 12–23.
[40] M. Zamir, S.M. Wrigley, B.L. Langille, Arterial bifurcations in the cardiovascular system of the rat, J. Gen. Physiol. 81 (1983) 325–335.
[41] S. Rodbard, Vascular caliber, Cardiology 60 (1975) 4–49.
[42] A. Kamiya, R. Bukhari, T. Togawa, Adaptive regulation of wall shear stress optimizing vascular tree function, Bull. Math. Biol. 146 (1984) 127–137.